



Article

The inner and backside solar flares

Ramy Mawad ¹

¹ Astronomy & Meteorology Department, Faculty of Science, Al-Azhar University, Nasr City, Cairo, 11488, Egypt; ramy@azhar.edu.eg
* Correspondence: ramy@azhar.edu.eg

Abstract: The Sun is a huge gaseous body. However, we cannot observe events in the inner Sun due to the convection zone opacity according to previous models. Therefore, the flares originate from the front surface of the Sun. But the current study relied on the distance distribution of X-Ray solar flares, which concluded that the inner layers have much lower opacity than expected. It is even less than what was expected by the latest models based on helioseismology. This means that the flares may originate from the solar interior or solar core, and perhaps from the backside surface, and even appear to us from the frontside surface. Which the re-estimate and correct the currently listed solar flare’s location is needed. Additionally, the flare’s distance illustrations the solar interior layers and appears their boundaries from the core to the photosphere. This method allows us to monitor the variation of the core’s radius with time. The model of the flare’s distance has been developed in current study. But this needs to redevelopment after re-estimating the solar flares locations.

Keywords: The Sun; Solar Flare; Solar Core; Solar Interior layers; Radiative Zone; Convection Zone

1. Introduction

Although the gaseous nature of the Sun, its interior can be known only through models. Other outer layers such as the photosphere, chromosphere, and corona, can be observed. Most solar phenomena are occurring on these upper layers, such as solar flares that appear in the chromosphere and photosphere.

The previous studies of the heliographical distribution of the solar flares were studied in different methods. [1,7,13,14,17,21] studied the latitudinal distribution. One of the previous studies on the solar flare’s location on the solar disk found that the solar flare’s latitude varies with the solar activity [2].

[5,9–11] studied the longitudinal distribution of the solar flares. The latitudinal and longitudinal distribution were studied together, and it was found that the solar flares occur in a specific latitude called “eruptive latitude” [13]. Most solar flares occur near or within active regions. Because these solar flares need magnetic energy.

The different layers in the sun can only be seen under certain conditions, or at certain bands. Except for the innermost layer of the sun’s atmosphere “photosphere”, it is the layer where most of the sun’s energy is, and always seen. We can observe it directly. Although the corona is the highest layer, it cannot be seen directly. But is it possible to observe the inner layers of the sun such as the solar core? or is it possible to observe the effect of the inner layers on the solar surface?

The produced energy in the solar core must pass through large amounts of plasma to reach the solar surface where it is radiated away by mainly two ways radiation and convection. The solar energy transport switches from radiation to convection. The transmission of this energy from the interior to the photosphere and appearance of interior layers depends on the opacity of the convection zone. Geometrically, we can see the inner layers of the sun as in figure 1. Because the direction of the observer penetrates the inner layers of the sun. Unfortunately, the models give high opacity for the convection zone [19]. So those inner layers can’t be seen. Modern studies such as [18,19] has been used helioseismology as an indication to what is inside the sun

Citation: Mawad, R. The inner and backside solar flares. *Journal Not Specified* **2022**, *1*, 0. <https://doi.org/>

Received:
Accepted:
Published:

Publisher’s Note: MDPI stays neutral with regard to jurisdictional claims in published maps and institutional affiliations.

Copyright: © 2022 by the authors. Submitted to *Journal Not Specified* for possible open access publication under the terms and conditions of the Creative Commons Attribution (CC BY) license (<https://creativecommons.org/licenses/by/4.0/>).



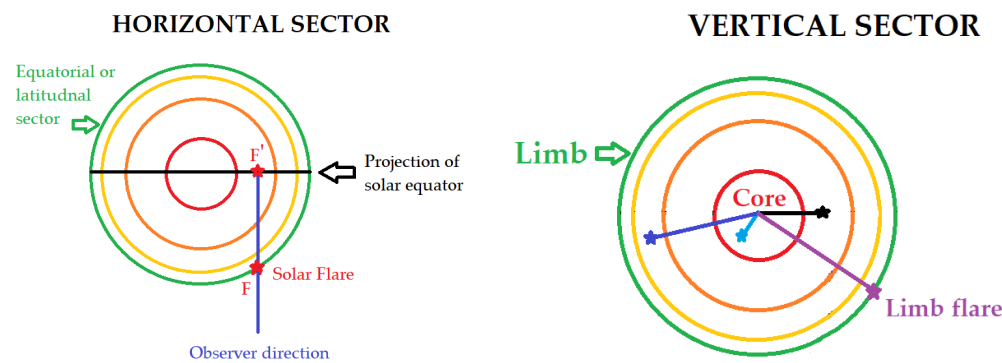


Figure 1. Plot (A): Equatorial and latitudinal section of the Sun (horizontal sector). The green circle represents to the solar latitude. The Black circle represents to the projection of the solar latitude on the solar disk. F is the solar flare on the spherical surface. While F' is the projection of the solar flare on the solar disk. Plot (B): The solar disk (vertical sector) of the sun. Turquoise line represents the distance D of the flare above the solar core. Consequently, it is above the rest of the inner layers. Black and indigo lines represent the solar flares above other inner layers such as radiative and convection zone layers. Purple line is the central distance of the solar flare above the solar limb.It represents the solar photosphere only.

In this study, I will study the location of the solar flares, to study whether it simulates the solar inner layers, like helioseismology, which is used to validate the solar models describing the solar interior layers. I will use the angular distance from the center of the solar disk, which reflects the inner layers of the sun.

2. Distance Distribution

As we can see in figure 1 (A) of the horizontal sector of the sun, we have a solar flare point (denoted to F) on the spherical surface of the sun. The point of the solar flare has an image in the solar disk in the background (denoted to F'), after penetration of the inner layers of the sun. while figure 1 (B) shows various locations for solar flares that occur on the solar disk.

Turquoise point is the solar flare occurring above the solar core. The Turquoise represents the central distance D of the flare from the solar center of the solar disk to the flare's location. Consequently, this flare is above the rest of the inner layers. Black and indigo pointer lines represent the central distance of the solar flares above other inner layers such as radiative and convection zone layers. Purple line is the central distance of the limb solar flare.It represents the solar photosphere only. It has an angular distance of 1 R_{\odot} . The question that arises is, do the observations of the solar flares represent point F? or F' that reflects different layers in the background? To answer this question, we need to distribute the solar flare according to the central angular distance (hereafter, distance or D). It is believed that solar flares might help us understand the solar interior. Most CMEs have outward directions nearly perpendicular to the solar surface, according to the cone model [8]. Therefore, the Earth will be influenced mostly by Halo-CMEs originating from the center of the solar disk, and not from the solar limb. While the solar flares' emission originating from any part of the solar disk will affect the geomagnetic field [15]. This is because the solar flare' emission moves in all directions, outward and may be inward as well. Considering the opacity of the convection zone is not complete, the solar flare may receive radiation from the inner layers. Could the positions of the solar flares reflect the inner layers? The distance distribution of solar flares may help us verify this assumption.

2.1. Distance calculation method

The main vital factor simulating the solar interior layers and projecting them on the solar disk is the distance of the solar flares. The estimation of distance is done by assuming

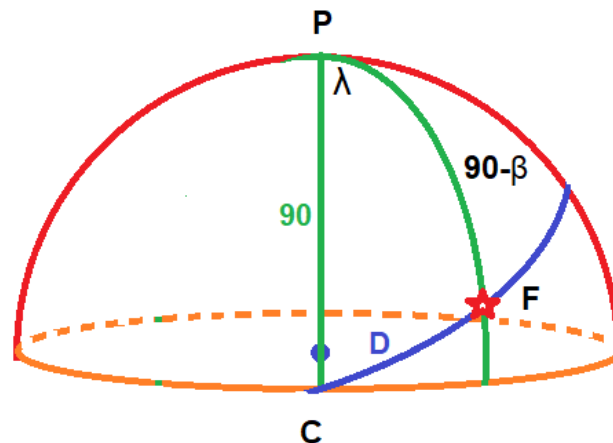


Figure 2. Spherical triangle of the projected solar flare F on the solar surface. While C denotes the center of the solar disk. This center is positioned on the solar equator (orange circle). The right green great circle is the flare's longitude pass from pole P, while the left green great circle line is the central meridian of the Sun. The arc CF is the angular distance between the center of the solar disk and the flare.

the Sun is a spherical body, using the laws of a spherical triangle, as shown in figure 2, by applying the cosine formula, the distance can be derived by the following formula:

$$D = \arccos [\cos(\lambda) \cos(\beta)], \quad (1)$$

Where D is the flare's distance between the projected center of the solar disk on the sphere and the solar flare heliographical location. β and α are the heliographical flare's latitude and longitude, respectively. We can divide the distance into 90 slices (interval) to give us a higher accuracy (i.e., 1° interval). This range will be 1-90. The smallest circle is the closest one to the center which simulates the solar core. The greater one is the circle at the limb.

3. Results and Discussions

The distance is calculated for all SXR during the period 1975-2021 obtained by GOES [20] and counted them according to their distance. In addition to RHESSI solar flares during the period of 2002-2021 for comparison.

Figure 3 (A) shows the result of the calculated distance for all flares during the selected period with their count of flares. This behavior of the curve indicates that the appeared flares are clearly illustrated the inner layers.

The central disk events are very few ($0 < D < 15$). This region reflects the solar core on the inner side. Also, the number of events is very low at the limb ($80 < D < 90$), which reflects the photosphere and chromosphere events only. While a large number of the flares happened at a distance of about 15° - 20° . This region denotes the inner side of the radiative zone after the projection of the solar core. Whereas the middle area ($20 < D < 80$) has a large number of X-ray events and this is because this region reflects many interior layers in the background.

The data is classified by solar cycle as shown in figure 3 (B), to check how the solar activity affects the curvature shape. We note that the curvature shape maintains the same as it is during each solar cycle (21 to 24 cycles).

Also, we can show about 4 peaks during the distance range 0 - 90° . The main and higher peak (hereafter, the core's peak) is a distance of about 15° - 20° that reflects the solar core. This means that the small peaks reflect other interior layers including radiative and convection zones, which we will discuss briefly.



Figure 3. The central distance distribution (D) of the X-Ray solar flare during all solar cycles (A Panel) and during each cycle (B panel) by the flare's count for GOES. While Plot C is for the RHESSI.

The core's peak moves and changes slightly with time. We notice that the distant radius is for cycles 21, 22, 24 then 23 respectively. This means that the solar core radius increases with increasing the strength of the solar cycle progress and activity, and vice versa.

It's worth noting that I repeated the same graph shown in figure 3 but classified data according to flares' classes (B, C, M, and X classes). Besides, I examined the solar activity by classifying data according to quiet and active periods for all the selected periods and during each cycle. I did not get a significant result. The curve of figure 3 remains similar.

The plot is applied with RHESSI solar flares during the same solar period as shown in figure 3 (C), to check how the solar radiation bands (X-Ray in current study) affect the curvature shape. I note that the curvature shape maintains the same as it is during distances $>1^\circ$. But the results gave a huge number of events in the middle of the solar disk (0°) with RHESSI data, unlike those observed by GOES. The number of flare events that have a distance greater than 1 is about 90,000. While we have about 25,000 flare events occurring at the center of the solar disk exactly.

For additional confirmation of this result, we can calculate the total importance I of these GOES flares that occurred at the same distance.

$$I_D = \sum(f_n/l), \quad (2)$$

Where f is the flare importance value. l is the importance of the solar flare, it equals 1 for X-Class, 10 for M-Class, 100 for C-Class, and 1000 for B-Class. m is the number of flare events that occurred at the same distance D . I_D is the total importance value in the X-Class unit that occurred in the distance D . Figure 4 shows the compatibility of the total importance with the number of events. But importance gives high contrast of the curvature peaks more than the count of the events. It is clear that we have 4 peaks similar to figure 2.

3.1. The radius of the inner layers

Figures 3 and 4 show four peaks after the core's peak, including two peaks after the convection zone. Each peak denotes an interior layer, and it has a boundary denoted by 2 crests. These crests appear clearly in weak solar cycles 23 and 24 especially in solar cycle 23. These peaks overlap during strong solar cycles such as 21 and 22. That longest distance demonstrates the radiative zone. The distance between the core and the radiative zone is not clear, because the curve is rising sharply within the solar core. The small peaks look unclear because they reflect different layers in the background with different projections and overlaps. In addition, it shows clearly that the inner layers' radii are compatible with previous studies. For comparable, the solar core-radiative zone boundary equals about $0.25 R_\odot$ according to previous studies [6,16]. While the radiation-convection boundary occurs at about $0.71 R_\odot$ [4]. Using equation 3, hence,

$$D_c = \arcsin(0.25) \simeq 15^\circ, \quad (3)$$

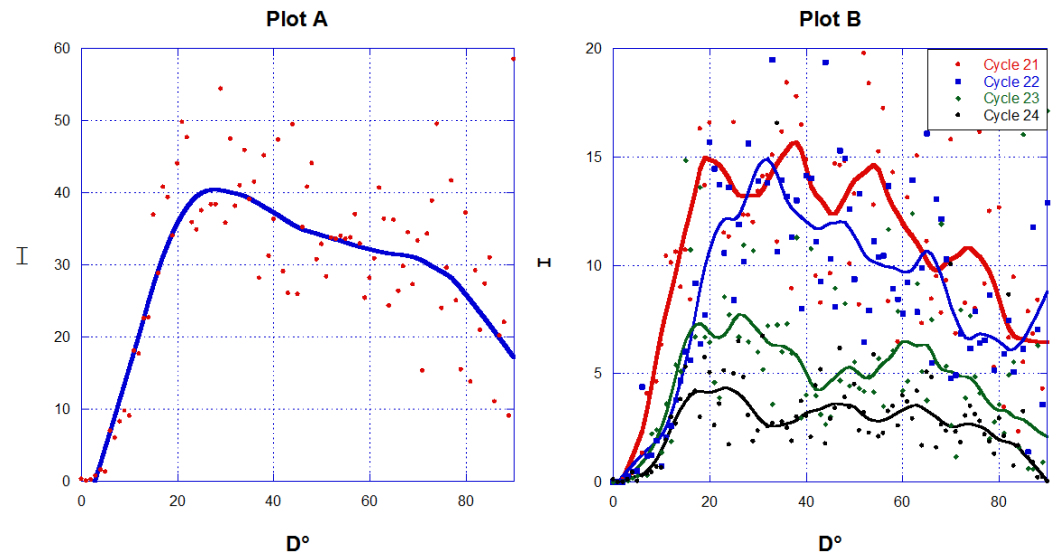


Figure 4. The central distance distribution (D) of the X-Ray solar flare during all solar cycles (A plot) during each cycle (B panel) by the flare's importance I in the X-Class unit.

$$D_r = \arcsin(0.71) \simeq 45^\circ, \quad (4)$$

$$D_v = \arcsin(0.81) \simeq 55^\circ, \quad (5)$$

Where θ_c , θ_r , and θ_v are the distance of the core, radiative zone, and convection zone. This result is compatible with current results demonstrated in figures 3 and 4, and the 15° distance represents the solar core (core's peak).

3.2. D relationship with solar depth

Previous studies calculated the radius of the inner layers in units of the radius of the sun R_\odot . It differs from the measurement method here in this study, which reflects the inner layers of the sun. So we need to convert the radius from scalar distance R_\odot to the angular distance D within the current study. So that the units are unified, it will be easier to compare the current results with the previous studies. The illustration in figure 5 shows the great circle CF sector of the Sun which is shown in figure 2. The black line is the projected solar diameter on the solar disk. It itself may be the solar equator if the position of the solar flare is on a solar equator. The distance D of any interior layer that has depth radius r is given by

$$\sin(D) = r/R_\odot \quad (6)$$

By putting the solar radius $R_\odot = 1$, then

$$D = \arcsin(r) \quad (7)$$

3.3. Distance Model

The first step is assuming the solar surface is a spherical body. The projection of the solar interior layers on the solar disk appears as circles around the center of the solar disk. We can split the Sun into 90 circles centralized by the center of the solar disk which appears as layers around the center of the solar disk. The suggested angular interval between these circles is 1° . We need to calculate the area of these projected circles on the real sphere in frontside and in the background including the backside too. If we calculated it for frontside, we could multiply it by n number for giving the areas of background spheres including backside. The projection of the circles on the real sphere is called "segment" which I want to estimate its area. Each segment has 2 bounders of circles, upper and lower. Each circle has central angles. θ is for the upper (far) circle and ϕ is for the lower (near) circle, which is

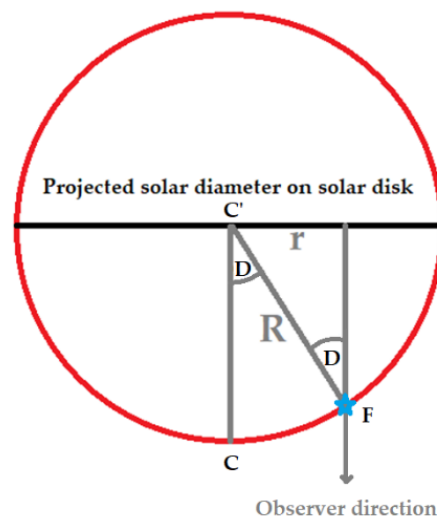


Figure 5. The scheme of the great circle CF as shown in figure 2.

measured from any flare's direction (point on this circle) and the center of the solar disk (direction to the Earth in heliographical coordinates), figure 6 illustrates this solar sphere the segment that we want to estimate its area.

The area of segment [22] is the difference between the boundary 2 caps. We can write

$$A = 2\pi R_{\odot}^2 [1 - \cos(\theta)] \quad (8)$$

Where A is the area of the frontside segment. Ω is the angular distance of the projected circle (segment angle). Then, the area of both spherical caps which have angles θ and $(\theta + 1^\circ)$ become

$$A_{\theta} = 2\pi R_{\odot}^2 [1 - \cos(\theta)] \quad (9)$$

$$A_{(\theta+1)} = 2\pi R_{\odot}^2 [1 - \cos(\theta + 1^\circ)] \quad (10)$$

The segment area formula become,

$$A = |A_{\theta} - A_{(\theta+1)}| = 2\pi R_{\odot}^2 [\cos(\theta) - \cos(\theta + 1^\circ)] \quad (11)$$

$$A = 2\pi R_{\odot}^2 [\cos(\theta) - \cos(\theta) \cos(1^\circ) + \sin(\theta) \sin(1^\circ)] \quad (12)$$

But $R_{\odot} = 1$, $\sin(1^\circ) \approx \frac{\pi}{180}$, and $\cos(1^\circ) \approx 1$ then

$$A \approx 2 \frac{\pi^2}{180} \sin(\theta) \quad (13)$$

Equation 13 refers to the sinusoid function. In order to integrate this segment area over all the background layers reaching to the backside of the photosphere, the equation becomes Summation of Sinusoids equation ([23]) that written as

$$I_D = v \sum_{n=1}^m (a_n \cos(D \times T_n)) \quad (14)$$

where a_n are the amplitudes represented an inner layer, T_n are the frequencies angels (period) in degrees. v is the offset value, and D is the distance of the solar flares of the solar flare count n or the summation of the importance in X-Class I of all solar flares that occurred in the same distance. I set $m = 3$ because this is the best value for the high correlation coefficient represents the simplest equation. With the examination of the compatibility of equation 14 with experimental data, it was found that equation 14 gives a strong coefficient

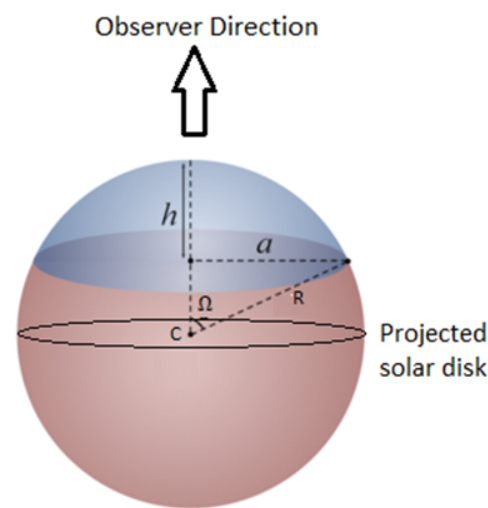


Figure 6. The schematic of the Sun. C is the center of the Sun and the solar disk. The black circle is the projected solar disk for the Sun for the observer. The spherical cap is the upper boundary of the spherical segment of the solar flares. The difference between areas of upper and lower caps gives a segment area.

of determination R^2 that is shown in table 1. R^2 equals 0.97 and 0.752 for the count and the importance of the flares. It was found that the sinusoid amplitude is greater than the value of $2\pi^2/180$ as in equation 14 which indicates that there are many layers in the background added to the front and back sides of the surface. The left panel of figures 5 and 3 shows the fitting curve.

Table 1. The Sum of Sinusoids fit parameters. R^2 is the coefficient of determination. v is the offset value. a is the amplitude. T is the period. P is the significance of the fit $P - test$. Chi-sq is the fitting error.

| N | Count | | Importance | |
|------------|-----------|---------|------------|---------|
| | A | T | A | T |
| 1 | -233.9 | 4.408° | -14.84 | 4.408° |
| 2 | -165.8 | 7.804° | -12.13 | 7.804° |
| 3 | -68.5 | 11.053° | -3.895 | 11.053° |
| v | 428.4 | | 28.82 | |
| R^2 | 0.97 | | 0.752 | |
| $Chi - sq$ | 1.099E05 | | 4059. | |
| P | 1.4266E67 | | 2.708E-29 | |

This result leads us to reconsider the estimation method of the solar flares coordinates because it considers that these events occurred only on the frontside of the solar surface. Besides, this equation is not accurate because it already depends on the current wrong recorded coordinate of the solar flares, which will need to be reformulated the equation latter after accurately estimating these coordinates.

4. Conclusions

With the study of the distance distribution of solar flares during the solar period 1975-2021 for GOES and during 2002-2021 for RHESSI, it turns out that this distance distribution can describe the inner layers of the Sun, similar to helioseismology. The distance curvature gives about 4 peaks during the distance range 0-90°. The main and higher peak is about 15°-20° which reflects the solar core. The small peaks reflect other interior layers including radiative and convection zones. The central disk events are very few ($0 < D < 15^\circ$) for GOES

flares and large for RHESSI. Also, the number of events is very low at the limb ($80^{\circ}<D<90^{\circ}$), which reflects the solar surface. While a large number of the flares happened at a distance of about 15° - 20° . This region denotes the inner side of the radiative zone after the projection of the solar core. Whereas the middle area ($20^{\circ}<D<80^{\circ}$) has a large number of X-ray events and this is because this region reflects many interior layers in the background. In addition, the solar core radius increases with increasing the strength of the solar cycle progress and activity, and vice versa. This result confirms that X-Ray solar flares at the surface are influenced by the inner layers and background emissions. This result is in agreement with previous studies of [20], who said that the two are correlated, almost certainly because of the increase in active region emission that coincides with increased flare occurrence; and with study of [12], who found that the present magnetic fields are probably deep-seated remnants of very ancient origin. This study also indicates that the solar flares's location are related to the direction of the observer.

Finally we concluded that:

- The measurements of solar flares vary according to the direction of the observer. So we need to re-measure the location (latitude and longitude) of the solar flares. We may need an additional satellite that monitors the same solar flare from another angle. So that we have two observations for the same solar flare, which help in knowing the correct coordinate of this flare;
- The soft X-rays which is observed in the solar flare may be from originated from the solar interior which is interacting with the surface radiation in the front side surface;
- The backside soft X-rays can not penetrate the solar core passing to the front side surface, Because of this, the central solar flare events most is a good choice to distinguish the front side solar flare events only from others. In addition, the limb solar flare events are represent only surface events;
- The Hard X-Ray has been detected in the center of the solar disk. It means that these hard X-Ray emissions come from the core of the Sun;
- I suggest that the solar atmosphere starts from the radiative zone and not from the photosphere.

Data Availability Statement: The X-ray solar flare data obtained by GOES satellites from the URL: https://hesperia.gsfc.nasa.gov/goes/goes_event_listings/ during the solar period 1975-2021 and by RHESSI from the URL: <https://hesperia.gsfc.nasa.gov/rhessi3/data-access/rhessi-data/flare-list/index.html>

Acknowledgments: The author thanks the teams of *GOES* and *RHESSI* for supporting the data that helped complete this study.
The author gives thanks to his mother, who supported him throughout her life to learning and serving humanity, and who asked Allah for success for me. I would also like to thank all my teachers.
I know that publishing this paper is difficult, because it contradicts with currently known concepts, and gives results opposite to those we knew before. In order to preserve my right and my desire to spread knowledge, I published this paper here at MDPI Preprints. For that, I thank the "MDPI Preprints" and all those in charge of it.

Abbreviations

The following abbreviations are used in this manuscript:

| | |
|----------|---|
| Distance | The Angular distance of the solar flare from the center of the solar disk |
| XSF | X-Ray solar Flare |

References

1.

Abdel-Sattar, Walid; Mawad, Ramy; Moussas; Xenophon: Study of solar flares' latitudinal distribution during the solar period 2002–2017: GOES and RHESSI data comparison, *Advances in Space Research* 62(9) 2701-2707, 2018. doi:10.1016/j.asr.2018.07.024

209

2.

Aschwanden et al., 2012

210

3.

Bornmann, P. L., Speich, D., Hirman, J., et al. 1996, in *GOES-8 and Beyond*, ed. E. R. Washwell, Vol. 2812, 291–298

211

4.

Christensen-Dalsgaard, J.; Gough, D. O.; and M. J. Thompson: The depth of the solar convection zone, *Astrophys. J.* 387, 413 (1991)

212

213

5. Cliver, E. W.; Mekhaldi, F. ; Muscheler, R., Solar Longitude Distribution of High-energy Proton Flares: Fluences and Spectra, *The Astrophysical Journal Letters*, 900(1), id.L11, 7 pp., 2020, DOI:10.3847/2041-8213/abad44 214

6. García, Rafael A. et al.; Tracking Solar Gravity Modes: The Dynamics of the Solar Core, *Science* 316 (5831), pp. 1591- (2007). doi:10.1126/science.1140598 215

7. Gnevyshev, M.N.: On the 11-years cycle of solar activity. *Sol. Phys.* 1(1), 107–120 (1967). <https://doi.org/10.1007/BF00150306> 216

8. Gopalswamy N.; Yashiro S.; Akiyama S., “Geoeffectiveness of halo coronal mass ejections”, *Journal of Geophysical Research* 112(A6), doi:10.1029/2006JA012149, 2007 217

9. Jetsu, L. search by orcid ; Pohjolainen, S. ; Pelt, J. ; Tuominen, I., 1996: Longitudinal distribution of major solar flares, Cool stars; stellar systems; and the sun : 9 : Astronomical Society of the Pacific Conference Series, volume 109; Proceedings of the 9th Cambridge workshop; held 3-6 October 1995 in Florence; Italy; *San Francisco: Astronomical Society of the Pacific (ASP)*; 1c1996; edited by Roberto Pallavicini and Andrea K. Dupree, p.135, 218

10. Li, Hongbo; Feng, Hengqiang; Liu, Yu ; Tian, Zhanjun ; Huang, Jin ; Miao, Yuhu, A Longitudinally Asymmetrical Kink Oscillation of Coronal Loop Caused by a Diagonally Placed Flare below the Loop System, *The Astrophysical Journal*, 881(2), article id. 111, 6 pp. (2019). 219

11. Loumou, K.; Hannah, I. G.; Hudson, H. S. , The association of the Hale sector boundary with RHESSI solar flares and active longitudes, *Astronomy & Astrophysics*, 618, id.A9, 12 pp., 2018, DOI:10.1051/0004-6361/201731050, arXiv:arXiv:1808.05866 220

12. Manuel, O.K., Ninham, B.W. & Friberg, S.E. Superfluidity in the Solar Interior: Implications for Solar Eruptions and Climate. *Journal of Fusion Energy* 21, 193–198 (2002). <https://doi.org/10.1023/A:1026250731672> 221

13. Mawad, Ramy; and Abdel-Sattar, Walid, “The eruptive latitude of the solar flares during the Carrington rotations (CR1986-CR2195)”, *Astrophysics and Space Science* 364: 197 (2019) doi:10.1007/s10509-019-3683-0 222

14. Pandey, K.K., Yellaiah, G., Hiremath, K.M.: Latitudinal distribution of soft X-ray flares and disparity in butterfly diagram. *Astrophys. Space Sci.* 356(2), 215–224 (2015). <https://doi.org/10.1007/s10509-014-2148-8> 223

15. Papaioannou A.; A. Belov; H. Mavromichalaki; E. Eroshenko; V. Oleneva, “The unusual cosmic ray variations in July 2005 resulted from western and behind the limb solar activity”, *Advances in Space Research* 43(4) 582-588 (2009). doi:10.1016/j.asr.2008.09.003 224

16. Ryan, Sean G.; Norton, Andrew J., *Stellar Evolution and Nucleosynthesis*, Stellar Evolution and Nucleosynthesis. *Cambridge University Press*, 2010. ISBN: 9780521196093 225

17. Shrivastava, P. K. & Singh, N.: Latitudinal Distribution of Solar Flares and Their Association with Coronal Mass Ejections, *Chinese Journal of Astronomy and Astrophysics*, 5(2), pp. 198-202 (2005). ADS: 2005ChJAA...5..198S 226

18. Thompson, Michael J; Helioseismology and the Sun’s interior, *Astronomy & Geophysics*, 45(4), August 2004, Pages 4.21–4.25, <https://doi.org/10.1046/j.1468-4004.2003.45421.x> 227

19. Turck-Chièze S et al 1993 Phys. Reports 230 57 Turck-Chièze, Sylvaine; Couvidat, Sébastien; 2011 *Rep. Prog. Phys.* 74 086901 228

20. Winter, L. M.; Balasubramaniam; K. S., 2014: Estimate of solar maximum using the 1–8 Å geostationary operational environmental satellites x-ray measurements, 2014 *ApJL* 793 L45. doi:10.1088/2041-8205/793/2/L45 229

21. Zharkova, V.V., Zharkov, S.I.: Latitudinal and longitudinal distributions of sunspots and solar flare occurrence in the Cycle 23 from the solar feature catalogues. In: Marsch, E., Tsinganos, K., Marsden, R., Conroy, L. (eds.) *Proceedings of the Second Solar Orbiter Workshop*. ESA-SP 641. *European Space Agency*, Noordwijk (2007). ISBN 92-9291-205-2. <http://adsabs.harvard.edu/abs/2007ESASP.641E..90Z> 230

22. Donaldson, Scott E.; Siegel, Stanley G. (2001). *Successful Software Development*. ISBN 9780130868268. Retrieved 29 August 2016. 231

23. Press, W.H., Teukolsky, S.A., Vetterling, W.T., Flannery, B.P.: *Numerical Recipes in C*. Cambridge University Press, Cambridge (1992) 232